

PAPER • OPEN ACCESS

Time evolution of quantum entanglement of an EPR pair in a localized environment

To cite this article: Jia Wang *et al* 2018 *New J. Phys.* **20** 053015

View the [article online](#) for updates and enhancements.

Related content

- [Signatures of the many-body localization transition in the dynamics of entanglement and bipartite fluctuations](#)
Rajeev Singh, Jens H Bardarson and Frank Pollmann
- [Manipulation of tripartite-to-bipartite entanglement localization under quantum noises and its application to entanglement distribution](#)
Xin-Wen Wang, Shi-Qing Tang, Ji-Bing Yuan *et al.*
- [Open-system dynamics of entanglement: a key issues review](#)
Leandro Aolita, Fernando de Melo and Luiz Davidovich

**PAPER**

Time evolution of quantum entanglement of an EPR pair in a localized environment

OPEN ACCESS**RECEIVED**

14 December 2017

REVISED


12 April 2018

ACCEPTED FOR PUBLICATION

16 April 2018

PUBLISHED

4 May 2018

Jia Wang¹ , Xia-Ji Liu and Hui Hu

Centre for Quantum and Optical Science, Swinburne University of Technology, Melbourne 3122, Australia

¹ Author to whom any correspondence should be addressed.E-mail: jiawang@swin.edu.au**Keywords:** many-body localization, entanglement, quantum memory

Original content from this work may be used under the terms of the [Creative Commons Attribution 3.0 licence](https://creativecommons.org/licenses/by/4.0/).

Any further distribution of this work must maintain attribution to the author(s) and the title of the work, journal citation and DOI.

**Abstract**

The Einstein–Podolsky–Rosen (EPR) pair of qubits plays a critical role in many quantum protocol applications such as quantum communication and quantum teleportation. Due to interactions with the environment, an EPR pair can lose its entanglement and no longer serve as a useful quantum resource. On the other hand, it has been suggested that introducing disorder into environment might help prevent thermalization and improve the preservation of entanglement. Here, we theoretically investigate the time evolution of quantum entanglement of an EPR pair in a random-field XXZ spin chain model in the Anderson localized (AL) and many-body localized (MBL) phase. We find that the entanglement between qubits decreases and approaches a plateau in the AL phase, but shows a power-law decrease after some critical time determined by the interaction strength in the MBL phase. Our findings shed light on applying AL/MBL to improve quantum information storage, and can be used as a practical indicator to distinguish the AL and MBL phase.

1. Introduction

An Einstein–Podolsky–Rosen (EPR) pair is a pair of qubits which are in a maximally entangled state. Due to their perfect quantum correlations, EPR pairs lie at the heart of many important proposals for quantum communication and computation, such as quantum teleportation [1, 2]. In reality, however, due to the unavoidable decoherence induced by coupling to the surrounding environment, an EPR pair might become a state ρ that loses entanglement after a certain time, making this qubit pair no longer useful as a quantum resource. One of the main tools to overcome the decoherence is a protocol named entanglement distillation [3, 4]. This method can be used to transform N_c copies of less entangled states ρ back into a smaller number m of approximately pure EPR pairs by using only local operations and classical communication (LOCC), where the ratio m/N_c depends on the amount of entanglement left in ρ . Therefore, it is of great interest to design quantum information storage devices that can keep a strong quantum entanglement for a long time to improve the distillation efficiency. In this work, we study the possibility of preserving quantum entanglement in a localized environment by introducing strong disorder.

The idea that disorder can help protect initial correlations and information is first proposed by Anderson in 1958. He focused on the behavior of non-interacting particles experiencing a random potential, which is now named as Anderson localization (AL) [5]. In AL, the diffusion of a particle's wave-packet in a disordered environment is absent, implying the initial information of the positions is 'remembered'. Extending this concept to an interacting system, namely many-body localization (MBL), has attracted many people's interest including Anderson himself. Recently, this field has attracted significant attention [6–8], partially due to the rapid progress in ultracold atomic experiments that has made quantum isolated many-body systems with tunable interaction and disorder available, including ultracold atoms in optical lattices [9–11] and ion traps [12]. These experimentally available systems constitute promising platforms for exploring the AL and MBL phases and stimulated a series of theoretical studies. Many remarkable properties of these localized phases have since been theoretically predicted: Poisson distributions of the energy gap [13, 14], absence of transportation of charge,

spin, mass or energy even at high temperature [15–17], protecting quantum order and discrete symmetry that normally only exists in the ground state [18–21], and existence of a mobility edge [22–24]. In particular, quantum entanglement has been discovered to play an important role in identifying different phases: energy eigenstates in localized phases have an area-law bipartition entanglement entropy, in contrast to the volume-law entropy of a thermalized state [25, 26]. In addition, after a sudden (global or local) quench, the entanglement shows a fast power-law spreading in a thermal phase, but only a slow logarithmic spreading in an MBL phase and no spreading at all in an AL phase [27–29]. The slow entanglement spreading in the localized phases is restricted by a variant of the Lieb–Robinson bound on the information light-cone, which can in principle be observed via out-of-time-order correlations (OTOC) [30–32]. This slow-spreading of entanglement also suggests that the local correlations might be maintained for a long time in a localized environment, which has a potential application in quantum information storage. Indeed, it has been shown that deep in the localized phase, the quantum coherence of local degrees of freedom, e.g. a single qubit, can maintain for a very long time [33, 34]. However, to the best of our knowledge, whether disorder can also help to protect quantum entanglement between qubits has never been directly studied. (The difference between behaviors of decoherence and entanglement in a localized environment is discussed in appendix C.)

In this work, we focus on studying the time evolution of the quantum entanglement between an EPR pair shared by two observers, namely Alice and Bob, and coupled to a localized environment. The rest of the paper is organized as follows. In section 2, the details of our model set-up to study this problem is outlined. The numerical results are reported in section 3 and an analysis of these results using ℓ -bit model are present in section 4. A summary of our study is given in section 5.

2. Model

As a concrete example, we conduct our analysis on a prototype Hamiltonian that has been studied extensively in the MBL literature: a one-dimensional $s = 1/2$ spin chain XXZ Hamiltonian with nearest neighbor interactions,

$$H = \sum_{i=1}^{L'} J(s_i^x s_{i+1}^x + s_i^y s_{i+1}^y) + \Delta s_i^z s_{i+1}^z + h_i s_i^z, \quad (1)$$

where J and Δ are the coupling constant, and h_i are random fields uniformly distributed over $[-h, h]$. The parameter L' that determines the upper limit of the summation can be used to conveniently implement open boundary condition or to decouple the last spin. The total magnetization $S_z \equiv \sum_i s_i^z$ is a good quantum number, and hence we will restrict our calculation for $S_z = 0$ hereafter (unless otherwise specified). We want to emphasize here that the spin–spin interacting Hamiltonian is chosen not only because its localized phase has been well studied, but also because in some cases, the main source of decoherence for qubits is from their interaction with unwanted environment spins. We also remark here that the Hamiltonian in equation (1) can be mapped onto a Fermi–Hubbard model using a Jordan–Wigner transformation, where J is equivalent to the hopping coefficient and Δ is equivalent to the interaction strength. Thus, with strong enough disorder h the spin chain is expected to be in the AL (MBL) phase for $\Delta = 0$ ($\Delta \neq 0$).

We prepare an initial state in the form of $|\Psi(0)\rangle = |\text{EPR}\rangle_{\text{AB}} \otimes |\text{NEEL}\rangle_{\text{E}}$ (unless otherwise specified), where the subscript A stands for Alice’s spin, B stands for Bob’s, and E stands for all the other spins serving as an environment. The environment is prepared in a Néel state mimicking a high-temperature environment and is initially *not* entangled with the EPR pair of the spins A and B. We then study the time evolution of this state under the Hamiltonian in equation (1) using exact diagonalization, obtaining the reduced density matrix ρ of the spin pair A and B by tracing out all the environment spins and calculating quantum entanglement measurements that are usually averaged over many realizations of disorder (typically 1000 times). The details of numerical calculation are given in appendix A. The quantum entanglement measurement we focus on here is the logarithmic negativity is given by $S_N = \log_2(N + 1)$, where the negativity N , is a measure related to the Peres–Horodecki criterion: $N = 2 \sum_i \max(0, -\mu_i)$ [35, 36]. Here, μ_i is the eigenvalues of ρ^Λ that is the partial transpose of ρ . We would like to remark here that the logarithmic negativity, even though lacks convexity, is a full entanglement monotone that does not increase on average under a general positive partial transpose preserving operation as well as LOCC [37]. In addition, the logarithmic negativity serves as the upper bound of distillable entanglement that limits the amount of nearly maximally entangled qubit pairs that can be asymptotically distilled from N_c copies of ρ [3, 4].

In our current set-up, two scenarios can be studied: in the first scenario shown in figure 1(a), Bob is isolated from the environment, which resembles a quantum communication or quantum teleportation situation; in the second scenario illustrated in figure 1(b), both Alice and Bob are in contact with the same environment mimicking a quantum calculation realization. To be specific, we usually put Alice’s (Bob’s) spin at the left (right) end of the chain, the initial state can thus be expressed explicitly as

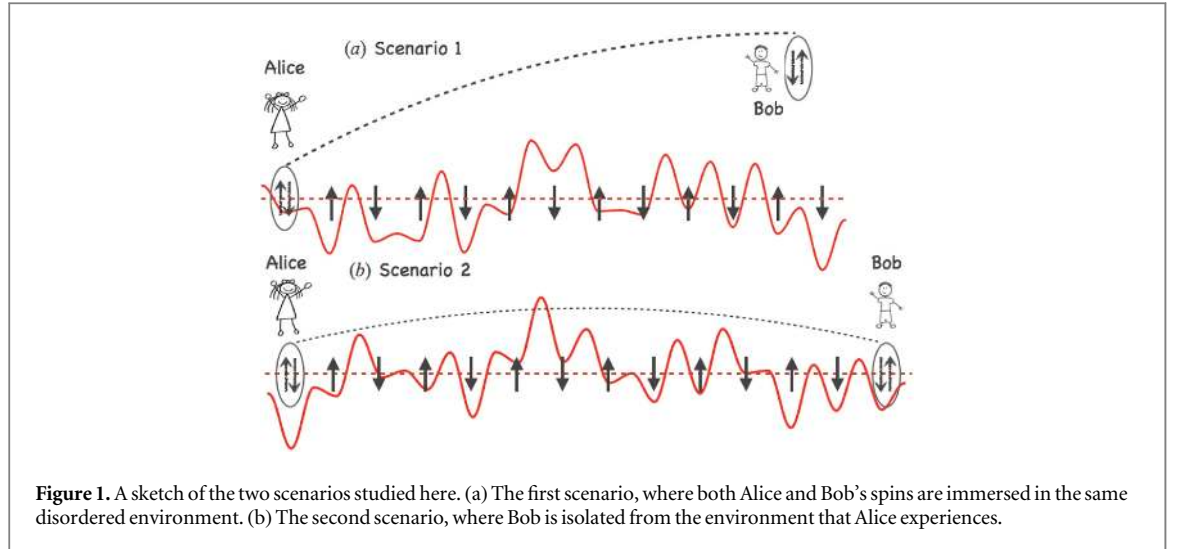


Figure 1. A sketch of the two scenarios studied here. (a) The first scenario, where both Alice and Bob's spins are immersed in the same disordered environment. (b) The second scenario, where Bob is isolated from the environment that Alice experiences.

$$|\Psi(0)\rangle = \frac{1}{\sqrt{2}}(|\uparrow\rangle_1 \otimes |\downarrow\rangle_L + |\downarrow\rangle_1 \otimes |\uparrow\rangle_L), \quad (2)$$

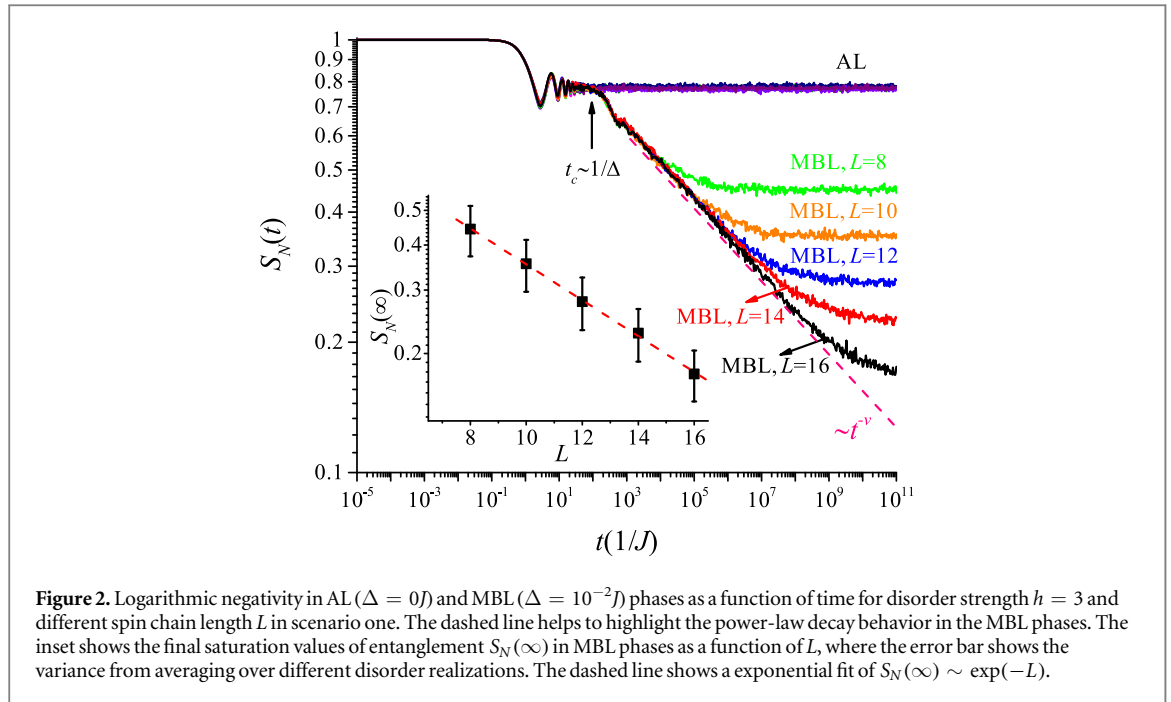
where the subscript gives the site number of the corresponding spin, and $c = 2, 3 \dots, L - 1$, where L is the number of sites in the spin chain. In scenario one, the last spin (Bob's spin) is decoupled from the system [$L' = L - 2$ in equation (1)] and experiences no on-site potential ($h_N = 0$); in scenario two, Bob's spin is coupled to the spin chain, and we set $L' = L - 1$ to implement the open boundary condition. Our numerical results show that the entanglement decreases in both scenarios and their evolution has similar qualitative behavior. The decrease of entanglement between Bob and Alice's spin can be understood by the monogamy properties of entanglement, i.e., a given spin that is maximally entangled with another spin cannot be entangled with any other spins. This implies that if Alice's spin is entangled with other spins in the spin chain, it can no longer form an EPR pair with Bob's spin. The spreading of entanglement in the spin chain causes the decrease of entanglement between Alice and Bob's spins. In addition, Bob's spin is completely decoupled from Alice's spin in scenario one; while in scenario two, Bob's spin is usually very far away from Alice's spin with no presence of long-range interaction. Hence, there is no or very little direct entanglement generation between Alice and Bob's spins in both scenarios, and the evolution of entanglement is mostly determined by the spreading of entanglement in the spin chain, which explains the similarity of entanglement evolution in the two scenarios. Hereafter, we focus on discussing the logarithmic negativity for scenario one. These discussion and conclusions are however applicable for other entanglement measurements such as concurrence and entanglement of formation in both scenarios. These details are discussed in appendix B.

3. Results

3.1. Entanglement evolution

Figure 2 shows our main result, the logarithmic negativity between Alice and Bob as a function of time in scenario one, with disorder strength $h = 3J$ for different numbers of spins L (including Alice and Bob's spins) and $\Delta = 0$ (10^{-2}) for the AL (MBL) phases. Initially, the entanglement is prepared at maximum $S_N(0) = 1$. At around $t \approx 1/J$, the entanglement in both AL and MBL phases shows a power-law decay following some oscillations, which has been recognized as the diffusion of an initial state to the size of the localization length. After a critical time $t_c \approx 1/\Delta$, the entanglement in the MBL and AL phases shows dramatically different behavior. The entanglement in AL phases converges to a constant value independent of the spin chain size L , where all curves for different L are visually overlapping. In contrast, the entanglement in the MBL phases shows a power-law decay $\sim t^{-\nu}$, with $\nu > 0$, which is emphasized by the linear behavior on a log-log scale in figure 2. Due to the finite size of our system, the entanglement in the MBL phases will eventually also saturate to some constant value after a significant time. Nevertheless, as illustrated in the inset of figure 2, the final saturated values are shown to decrease exponentially as a function of spin chain size $\sim \exp(-\beta L)$, where β is a constant.

From these observations, one can expect that the entanglement in AL phase will never reduce to zero, but become a constant depending only on disorder strength even in the thermodynamic limit $L \rightarrow \infty$. On the other hand, no matter how small the interaction strength Δ is, the entanglement will be dissipated after an infinitely long time in the thermodynamic limit. However, this dissipation is very slow if the disorder is strong enough. In addition, the entanglement of the AL phase and MBL phases only becomes different after the critical time t_c . If Δ is small, the entanglement in the MBL phase can still be preserved before t_c .

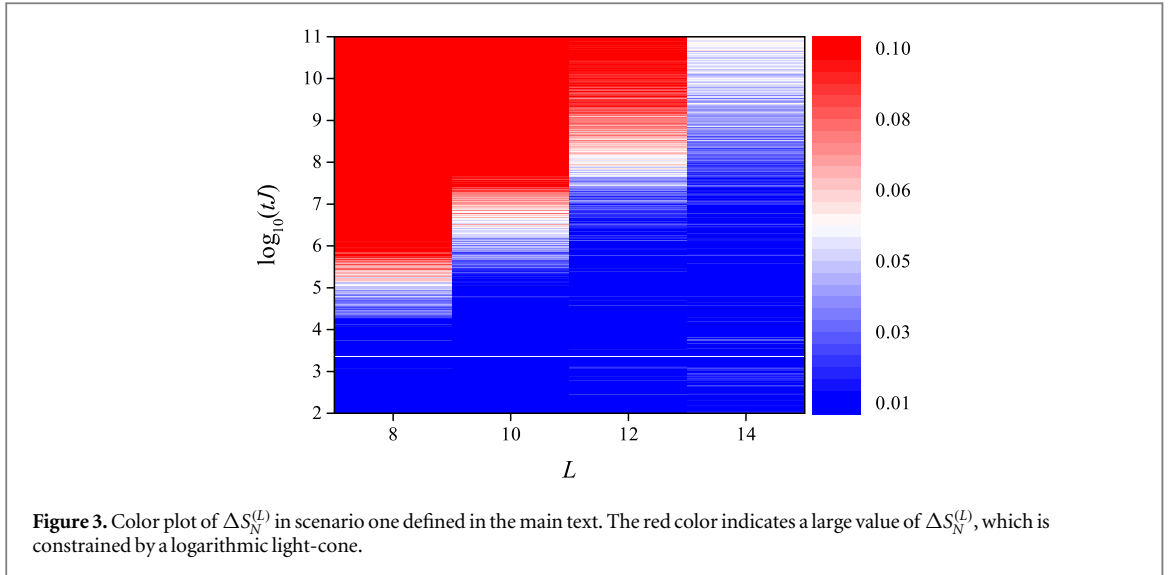


We can conclude that the AL phase is ideal for creating quantum storage devices to preserve quantum entanglement between a qubit pair. On the other hand, if a weak interaction strength Δ is unavoidable in the system, the MBL phase can still be applied to preserve entanglement with an expiration time t_c . After carrying out an entanglement distillation [3, 4], the qubit pair is then ready for quantum communication or teleportation. We also wish to emphasize here that the preservation of entanglement between two qubits in a localized environment is, of course, not better than in a completely decoupled environment. However, in a realistic situation where coupling between the qubit pair and the environment cannot be eliminated, our study provides a generic way of preserving entanglement without a specific fine tuning of the Hamiltonian but simply introducing strong enough disorder into the environment. For example, the main source of decoherence for nitrogen-vacancy (NV) centers in diamond are their interaction with randomly distributed ^{13}C nuclear spins [7]. We note that the NV centers have already been applied to make quantum memory [38], therefore our proposal to introduce disorder in nearby spins can be regarded as an improvement of the quantum memory.

Our results can also be directly applied to identify the localized phase being AL or MBL. Most previous such studies have focused on studying the bipartite entanglement, i.e. dividing the system into two sub-systems, of an initial product state after a global quench or an energy eigenstate after a local quench [27–29]. The experimental observation of bipartite entanglement in principle can be very challenging for a large system, and may even be impossible in the thermodynamic limit. On the other hand, measuring entanglement between local degrees of freedom in an optical lattice [39] and trap ions [40, 41] has been recently explored, motivating the studies of entanglement between local sites, where the entanglement between local degrees of freedom is more experimentally accessible [42–44]. These studies usually focus on the case where the initial state is a product state and a temporary entanglement generated due to initial diffusion. The AL and MBL features are analyzed by the decay of this temporary entanglement that is decreasing exponentially as a function of distances between sites in the deep localized phase. Therefore, these studies are usually limited to entanglement between nearest few sites. Our methods, using an initial prepared EPR pair, can in principle overcome these limitations and be experimentally accessible.

3.2. Logarithmic light-cone

Our study also gives an interesting insight into the nature of entanglement spread in MBL phases. The power-law decay and the saturated values of entanglement in MBL phases suggest that we can define a saturation time scale t_s , where the entanglement in MBL phases is saturating, as $\nu \log(t_s) \sim L$, which resembles the logarithmic light-cone found in previous bipartite entanglement studies [27–29]. This logarithmic light-cone can be understood from the modified Lieb–Robinson bound of information spreading (in this case entanglement spreading) in systems with short-range interactions [45]. One convenient and common way to describe the Lieb–Robinson bound is to compare the time evolution of a local observable A (at site i_A) under the full Hamiltonian H with its time evolution under a truncated Hamiltonian H_L , which only includes interactions contained in a region of distance no more than L . Under certain assumptions, a modified Lieb–Robinson bound



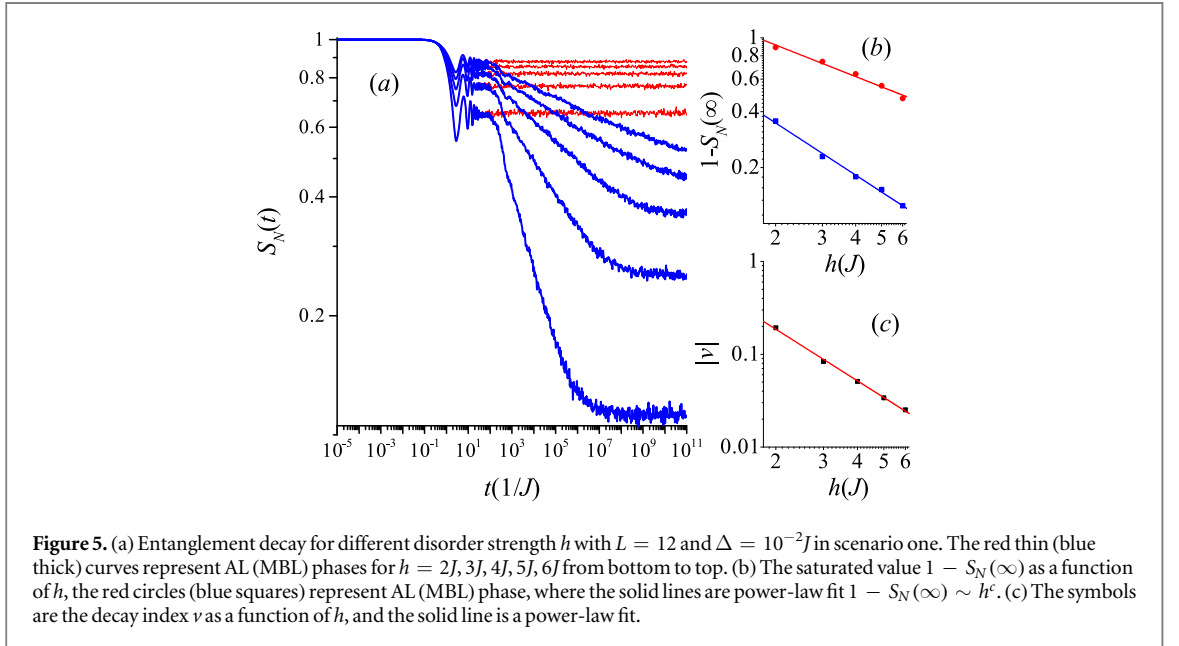
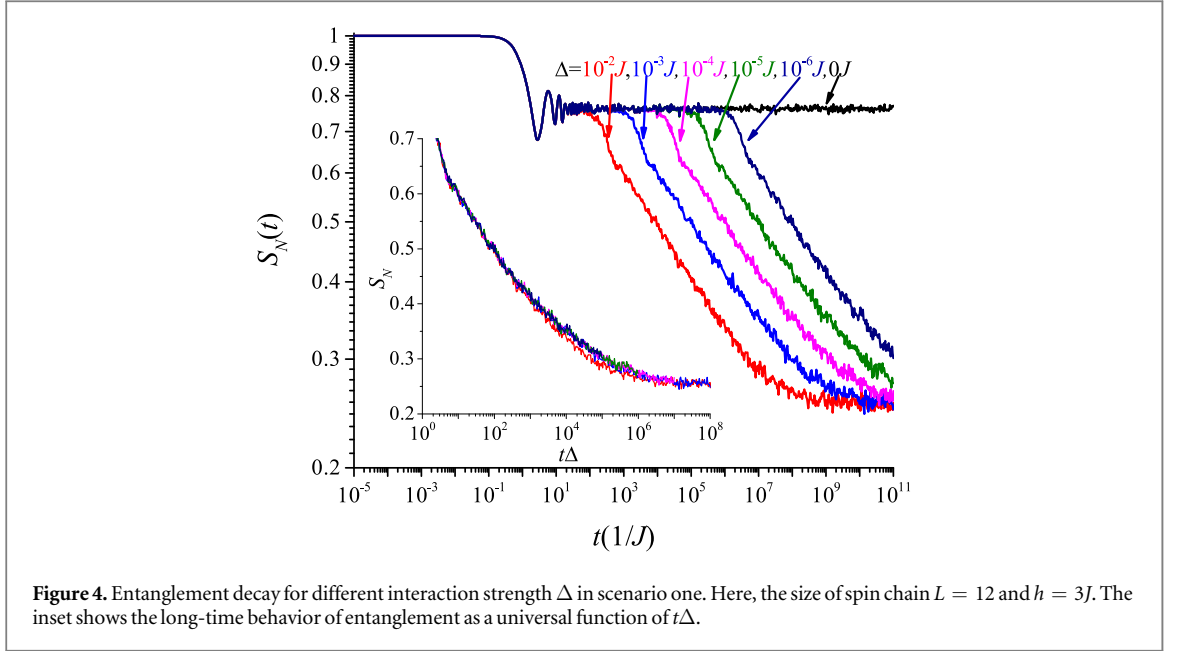
$|A(t) - A^{(L)}(t)| \leq at e^{-L/v} = ae^{-(L-v \log t)/v}$ has been proposed for MBL systems [46], where $a, v > 0$ are all constants, $A(t) = \langle \psi(0) | e^{iHt} A e^{-iHt} | \psi(0) \rangle$ and $A^{(L)}(t) = \langle \psi(0) | e^{iH_L t} A e^{-iH_L t} | \psi(0) \rangle$. The underlying physics is clear: at time t the degrees of freedom outside the light-cone is not entangled with the degrees of freedom at i_A . Therefore, the time evolution of observable A can be approximated by only considering the effects of the degrees of freedoms within the light-cone.

Even though entanglement is technically not an observable, we study the quantity $\Delta S_N^{(L)} = S_N^{(L=16)} - S_N^{(L)}$ in scenario one under the same spirit as Lieb–Robinson bound. Here, we choose to study the total Hamiltonian H with 16 spins. Since Bob’s spin is completely decoupled from the spin chain, the truncated Hamiltonian H_L only includes spins that are within the distance L to Alice’s spin at the leftmost site, which is equivalent to a spin chain Hamiltonian with only L spins. The quantity $\Delta S_N^{(L)}$ can be interpreted as the difference of entanglement evolution between a full spin chain of $L = 16$ and a truncated spin chain of $L < 16$ near Alice’s spin. The results are shown in figure 3, where one can directly see that the significant differences are constrained within a logarithmic light-cone. This is direct evidence that entanglement is spreading logarithmically in an MBL phase as suggested by previous OTOC studies [30–32].

3.3. Effects of disorder and interaction strength

We further take a qualitative analysis of the effects of interaction strength Δ and disorder strength h on the decay of entanglement. Figure 4 shows the entanglement decay for different Δ , confirming that entanglement in the AL and MBL phases only become different abruptly after the critical time $t_c \approx 1/\Delta$. Furthermore, the saturated value in the MBL phases does not vary appreciably for different Δ . In fact, the logarithmic entanglement for $t \gg t_c$ is a universal function of $t\Delta$ as shown by the inset of figure 4. Interestingly, the average two-site entanglement of a spin chain that is initially prepared in a product state also decays in time as a power-law in the MBL phase. However, the power-law exponent is not universal and displays a clear dependence on the interaction strength [43]. We believe that this is due to the average two-site entanglement including entanglement from neighbor sites that are directly coupled by the Ising interaction. The Ising interaction not only causes the spread of entanglement but also directly generate entanglement between the neighbor sites. In contrast, Bob’s spin is completely decoupled from Alice’s spin (and all the other spins in the chain) in our scenario one, therefore the decay of entanglement between Alice and Bob only reflects the spread of entanglement in the spin chain. Therefore, we conclude that the spread of entanglement is universal and independent of Δ , while the generation of entanglement between neighbor sites by Ising interaction depends on the interaction strength.

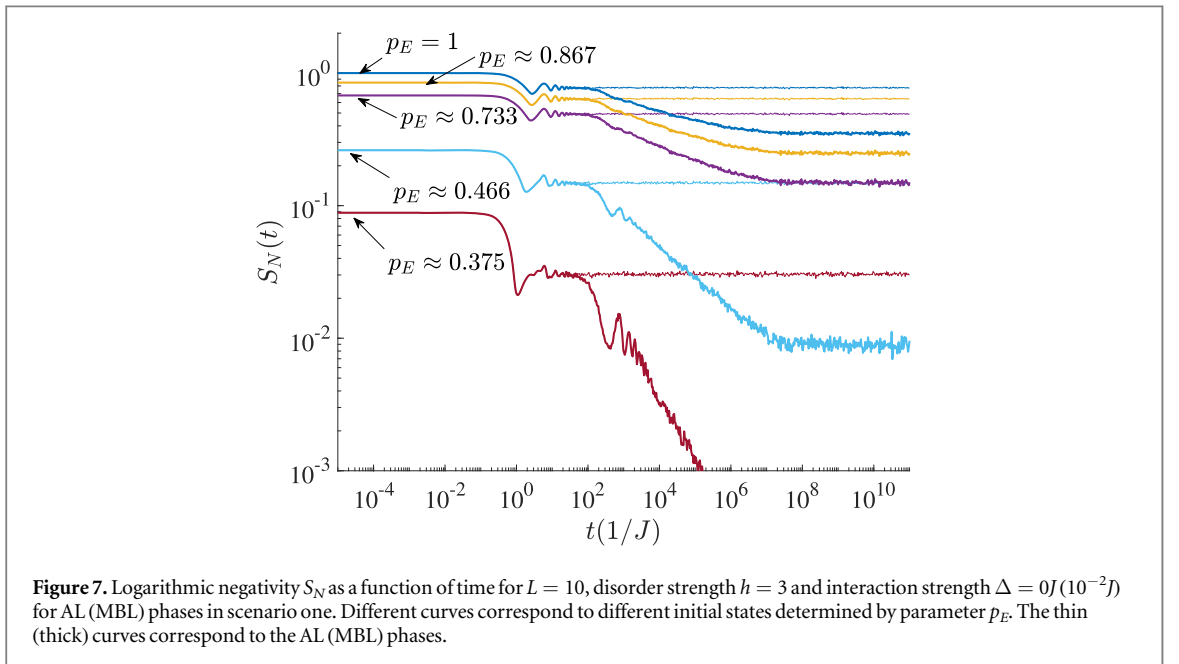
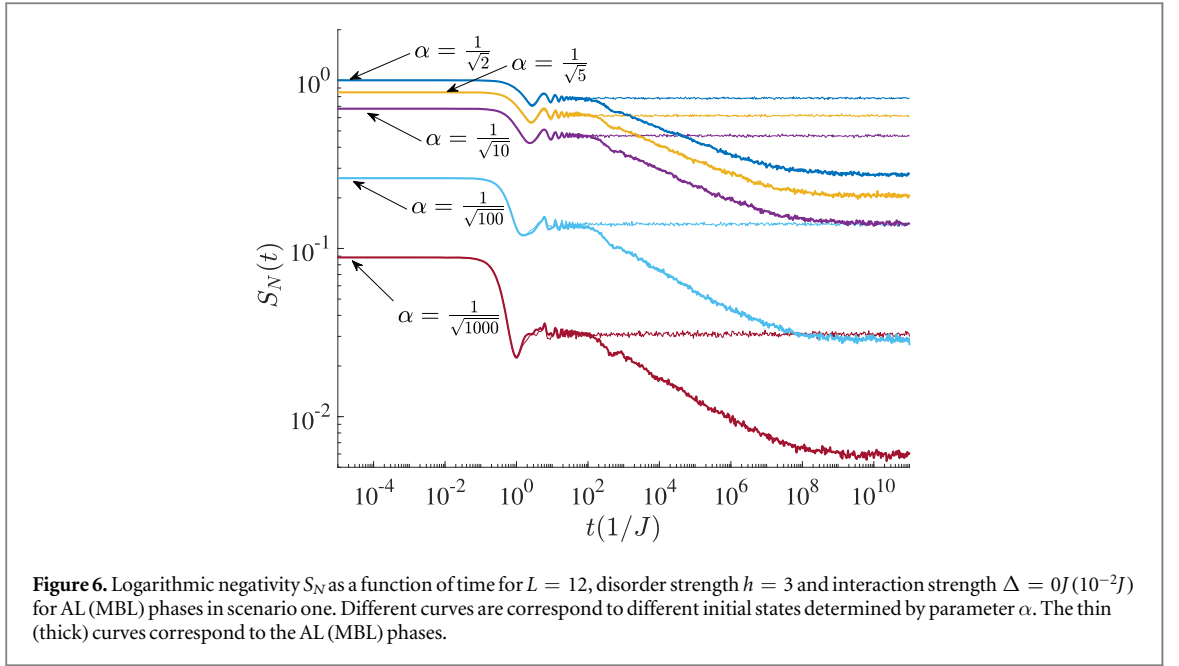
Finally, figure 5(a) shows the entanglement decay for different h , where the decay rate becomes slower and the saturated value becomes larger for a stronger disorder. As a result of the competition of these two effects, the saturation time becomes longer, suggesting that a stronger disorder is beneficial for storing EPR pairs. Our numerical results also show that the decrease of entanglement at infinite long time $1 - S_N(\infty)$ and the decay index ν both have a power-law dependence on h , as shown in figures 5(b) and (c). This analysis can be interpreted as a stronger disorder and weaker interaction is beneficial for preserving quantum entanglement, which is consistent with our expectation.



3.4. Non-maximally entangled state

Previous subsections focus on the situation where Alice and Bob's spin form a maximally entangled EPR pair initially. However, a perfect EPR pair might be challenging to prepare and fragile to manipulate. In this subsection, we show that the entanglement evolution is also qualitatively similar for non-maximally entangled initial state, and hence ensure the robustness of our scheme of preserving entanglement and distinguishing AL/MBL phases. We first study the case of non-maximally entangled state, $|\Psi(0)\rangle = |\Phi_\alpha\rangle_{AB} \otimes |\text{NEEL}\rangle_E$, where $|\Phi_\alpha\rangle_{AB} = \alpha|\uparrow\downarrow\rangle + \beta|\downarrow\uparrow\rangle$ and $|\alpha|^2 + |\beta|^2 = 1$. The initial negativity and logarithmic negativity is therefore given by $N(0) = 2|\alpha||\beta|$ and $S_N(0) = \log_2(2|\alpha||\beta| + 1)$, respectively. When $\alpha = \beta = 1/\sqrt{2}$, the system reduced to the EPR pair case. We can also study the case where the initial state is a mixed state $\rho(0) = \rho_{AB}(0) \otimes |\text{NEEL}\rangle_{EE} \langle \text{NEEL}|$, where we choose $\rho_{AB}(0) = p_E |\text{EPR}\rangle_{ABAB} \langle \text{EPR}| + (1 - p_E) I_{AB}/4$. $\rho_{AB}(0)$ can be regarded as the convex combination of a maximally entangled state, $|\text{EPR}\rangle_{AB}$, and a maximally mixed state, I_{AB} . The initial negativity and logarithmic negativity can also be given analytically as $N(0) = (3p_E - 1)/2$ and $S_N(0) = \log_2(3p_E/2 + 1/2)$, respectively. When $p_E = 1$, $\rho_{AB}(0)$ reduces to an EPR pair, and when $p_E \leq 1/3$, $\rho_{AB}(0)$ becomes separable.

Figures 6 and 7 show the time evolution for different initial pure $|\Phi_\alpha\rangle_{AB}$ and mixed state $\rho_{AB}(0)$, respectively. These results show that the quantitative behavior of the entanglement evolution are quite similar regardless of



whether the initial state is maximally entangled or whether it is pure. For $t > t_c$ the entanglement has a power-law decay in the MBL phase and approaches a constant value in the AL phase. While the power-law exponent in the MBL phase and the constant value in the AL phase depend on the details of Hamiltonian, for the purpose of identifying AL/MBL phases, our scheme is robust with respect to the different initial states. We also remark here that, if the initial state $\rho_{AB}(0)$ is separable, i.e. $p_E \leq 1/3$, Alice and Bob's spin will always remain separable in scenario one (not shown in the figures here). This can be understood by realizing that Bob's spin is not coupled to Alice's spin or any other spins in the spin chain. If they are initially separable, there is no mechanism to create entanglement between them.

4. Discussion

In this section, we intend to understand the power-law decay of entanglement in another perspective by studying the same physics in an effective phenomenological model, i.e., the ℓ -bit model [47]. In the deep localized regime,

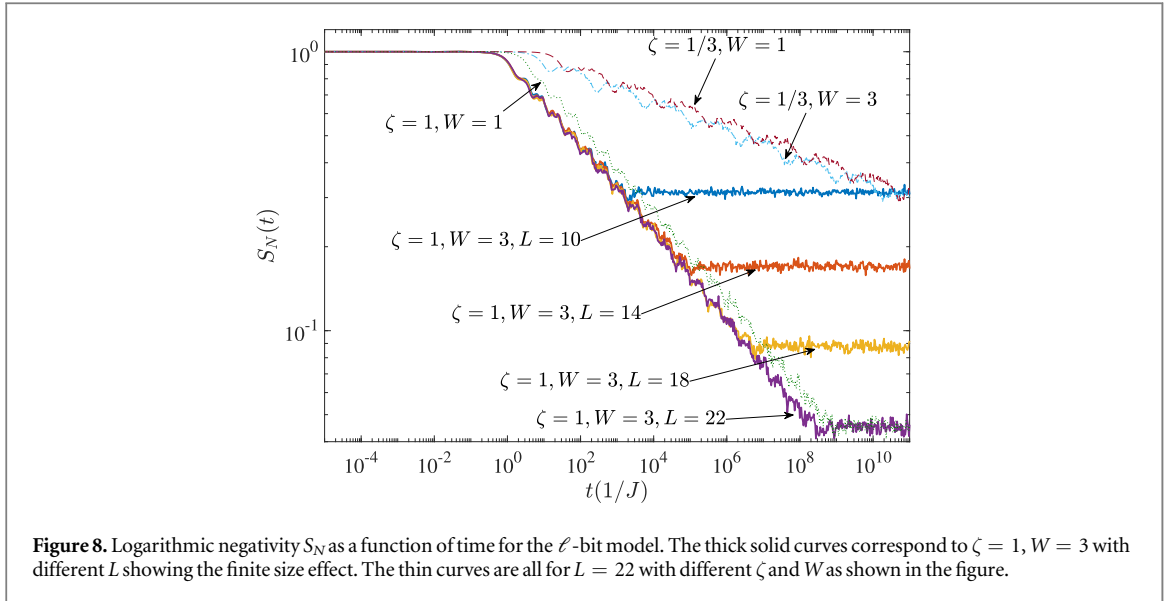


Figure 8. Logarithmic negativity S_N as a function of time for the ℓ -bit model. The thick solid curves correspond to $\zeta = 1, W = 3$ with different L showing the finite size effect. The thin curves are all for $L = 22$ with different ζ and W as shown in the figure.

the system possesses an extensive number of locally conserved quantum numbers (‘constants of motion’). One can in principle construct local operators corresponding to these conserved quantum numbers and define them as local pseudospins $\{\tau_i\}$, namely ℓ -bits (localized-bits), in contrast to the p-bits $\{s_i\}$ (physical spins). One intuitive way to construct τ_i is to suitably dress s_i at the same site with nearby p-bits so that the Hamiltonian can be written in the form,

$$H_\ell = \sum_i \tilde{h}_i \tau_i^z + \sum_{i,j} \tilde{J}_{ij} \tau_i^z \tau_j^z + \dots, \quad (3)$$

where \tilde{h}_i are random fields and $\tilde{J}_{ij} = W_{ij} e^{-|i-j|/\zeta}$ are interaction terms, with \tilde{h}_i and W_{ij} both assumed to be random variables uniformly distributed in the range $[-W, W]$, and ζ is a constant that should be determined by the localization length. Further terms in H_ℓ only include $n > 2$ products of τ_i^z s, but no terms involving τ_i^x or τ_i^y may appear. For simplicity, the higher order terms will be neglected and are irrelevant for our purposes. The dynamic of ℓ -bits under H_ℓ is clear: all ℓ -bits precess about the z-axes of their Bloch sphere with conserving τ_i^z s. The rate of precession is however determined by all τ_i^z s (with the effects of ℓ -bits at long distance suppressing exponentially), which leads to dephasing.

Inspired by [43], we study the ℓ -bit model numerically to see the effects of dephasing. The precise form of the mapping between $\{\tau_i\}$ and $\{s_i\}$ is not obvious, but in general, an EPR pair in p-bits cannot be directly mapped to an EPR pair in ℓ -bits. Nevertheless, we focus here on the explanation of power-law decay in MBL phase that exists regardless of the form of initial state as long as there is entanglement. Therefore, we choose to study the evolution of entanglement of an initial EPR pair in ℓ -bits $|\Psi(0)\rangle = |\text{EPR}\rangle_{AB} \otimes |\Phi_0\rangle_E$, where

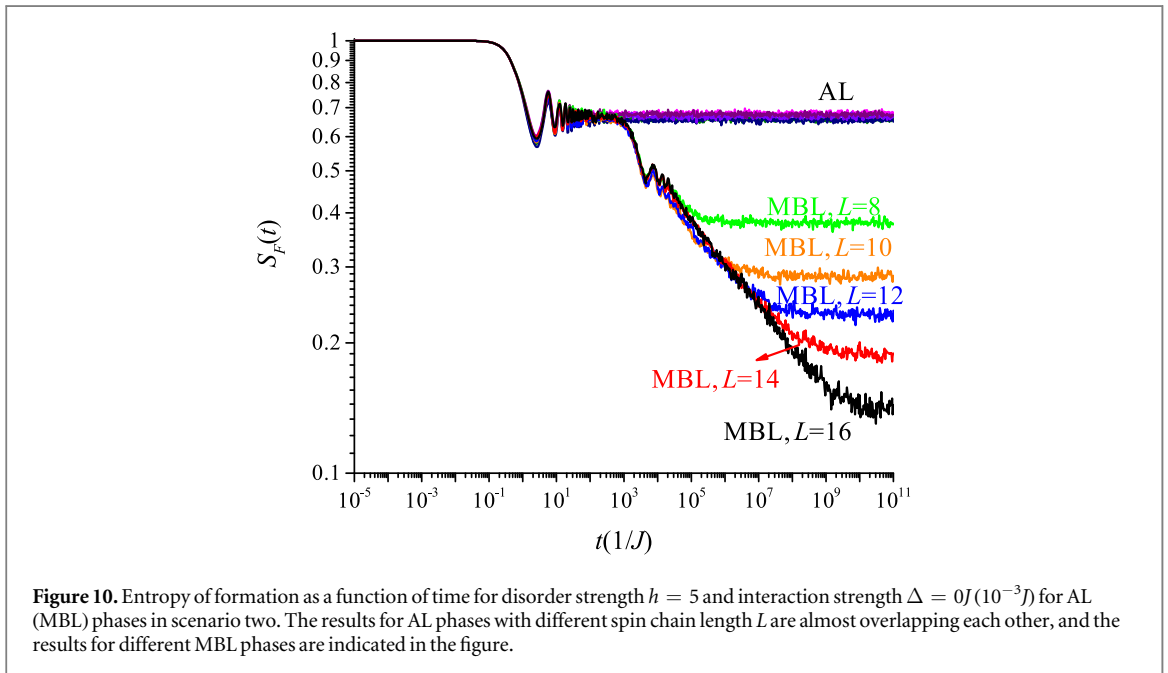
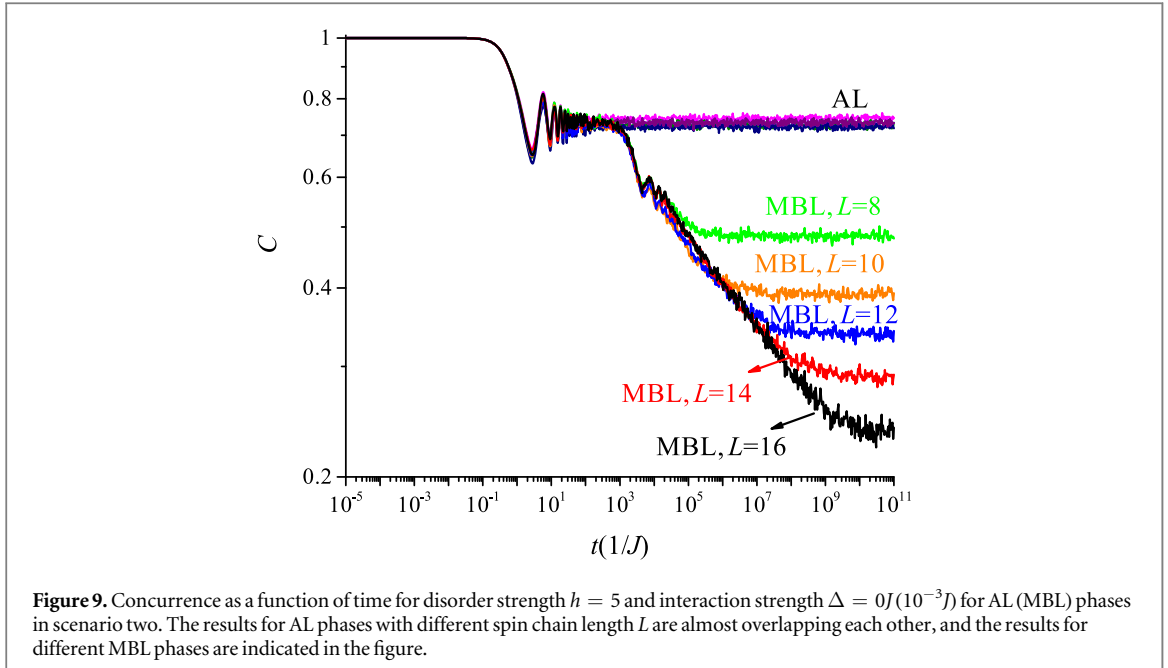
$$|\Phi_0\rangle_E = \otimes_{j=2}^{L-1} [\cos(\phi_j)|\uparrow\rangle + e^{i\theta_j} \sin(\phi_j)|\downarrow\rangle] \quad (4)$$

with θ_j and ϕ_j assumed to be random variables uniformly distributed in the range of $[0, \pi/2]$ and $[0, 2\pi]$, respectively. Similar to the scenario one we studied before, we assume Alice (Bob) have the leftmost (rightmost) ℓ -bit, and Bob’s ℓ -bit is completely decoupled from all the other ℓ -bits (including Alice’s). The calculation is averaged over 1000 distinct initial states (different realizations of $\{\theta_j\}$ and $\{\phi_j\}$), local disorder \tilde{h}_i and interaction terms W_{ij} .

Figure 8 shows the power-law decay of entanglement in the ℓ -bit model, where the final saturated constant is a finite size effect. It is also interesting to see that the power-law exponent seems to be independent of W but only determined by ζ .

5. Summary

In summary, we have studied the time evolution of quantum entanglement of an EPR pair coupling to a localization environment. This study allows us to explore the possibility and limitation of applying localization phase to preserve quantum entanglement between qubit pairs. Our results can also be regarded as an experimentally accessible protocol to discriminate AL and MBL phases, and understand the nature of entanglement propagation in these systems.

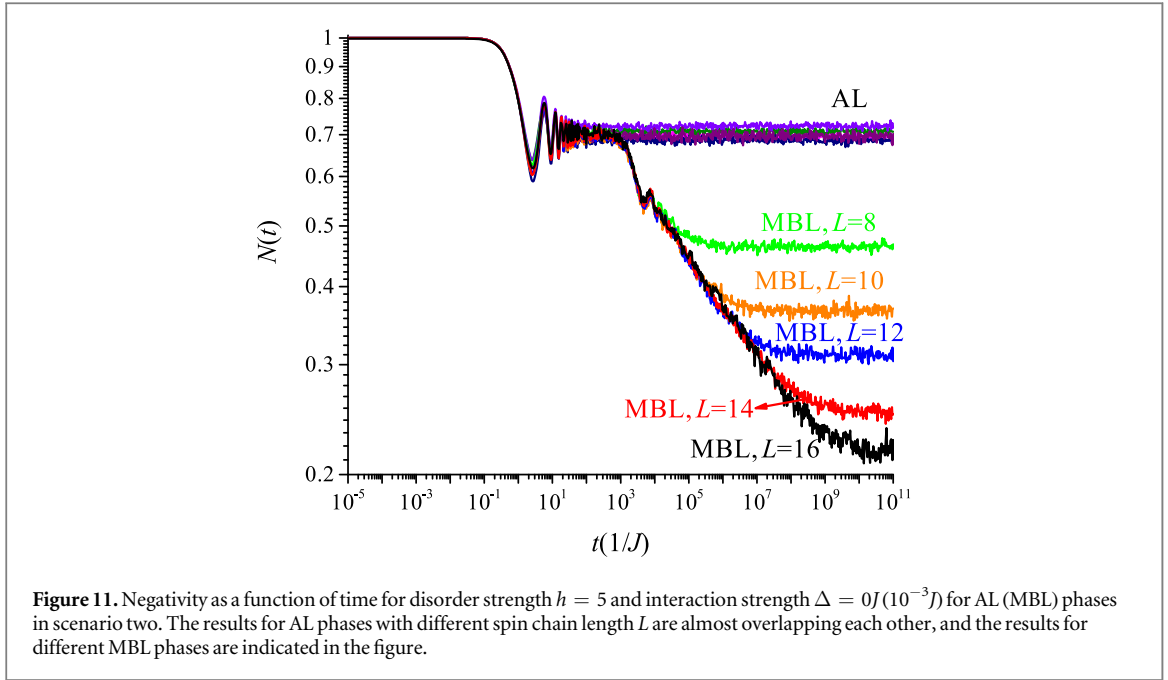


Acknowledgments

This research was supported under the Australian Research Council's Future Fellowships funding scheme (project number FT140100003) and Discovery Projects funding scheme (project number DP170104008). The numerical calculations were partly performed using Swinburne new high-performance computing resources (Green II).

Appendix A. Numerical methods

Since we are interested in the dynamic properties of the system in the thermodynamic limit at a very long time, ideally we would like to study systems with infinite size that evolve for infinite long time. But in reality, we can only work with finite size systems in a finite time and extrapolate our expectation to infinite size and time. Obviously, we would like to study the largest system that evolves for long enough time. The long-time limit makes propagation method such as split-operator or Crank–Nicolson method, where the accuracy propagation is limited by finite step size. Therefore, we use the conventional exact diagonalization method, where we



diagonalized the Hamiltonian and get all the eigenstates $|\psi_\beta\rangle$ and eigenenergies E_β . The time evolution of the quantum state $|\psi(t)\rangle$ is then described by a projected wavefunction

$$|\psi(t)\rangle = \sum_{\beta} \langle \psi_\beta | \psi(0) \rangle e^{-iE_\beta t},$$

where the accuracy is then only limited by the machinery accuracy of $|\psi_\beta\rangle$ and E_β , allowing us to evolve our system to very long time. However, the exact diagonalization for all eigenpairs is limited by the system size and computation power. In the future, we intend to apply the more advanced time-evolving block-decimation technique that based on matrix product state and density matrix renormalization group to access larger systems.

Appendix B. Quantum entanglement measurements

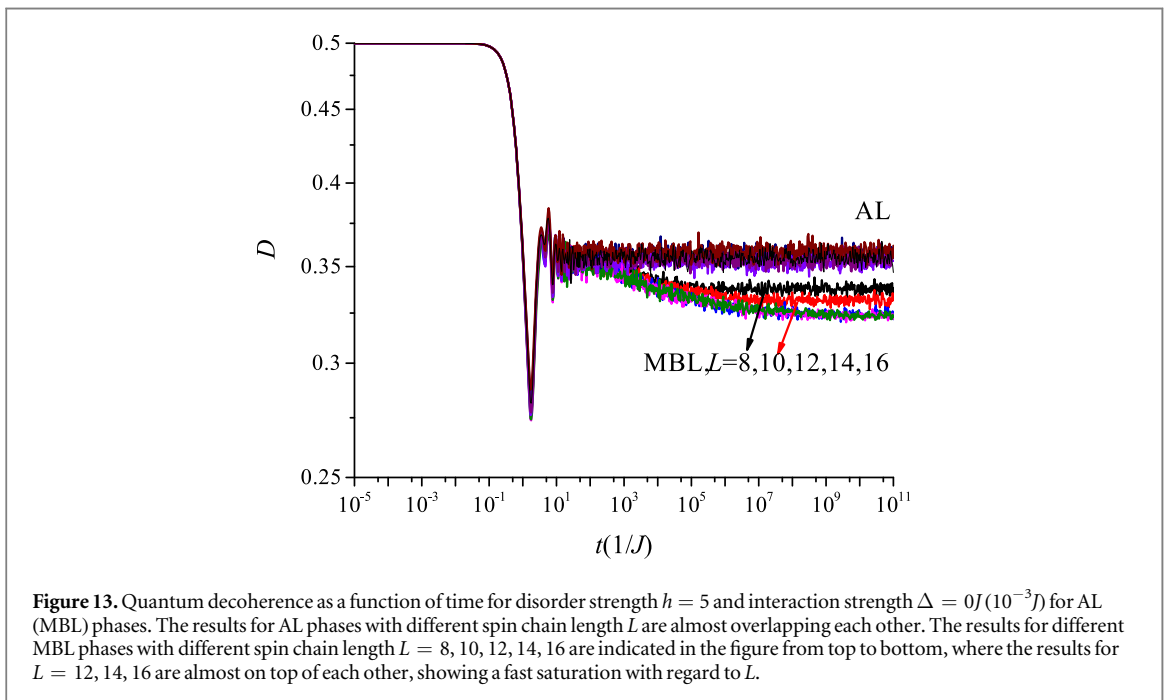
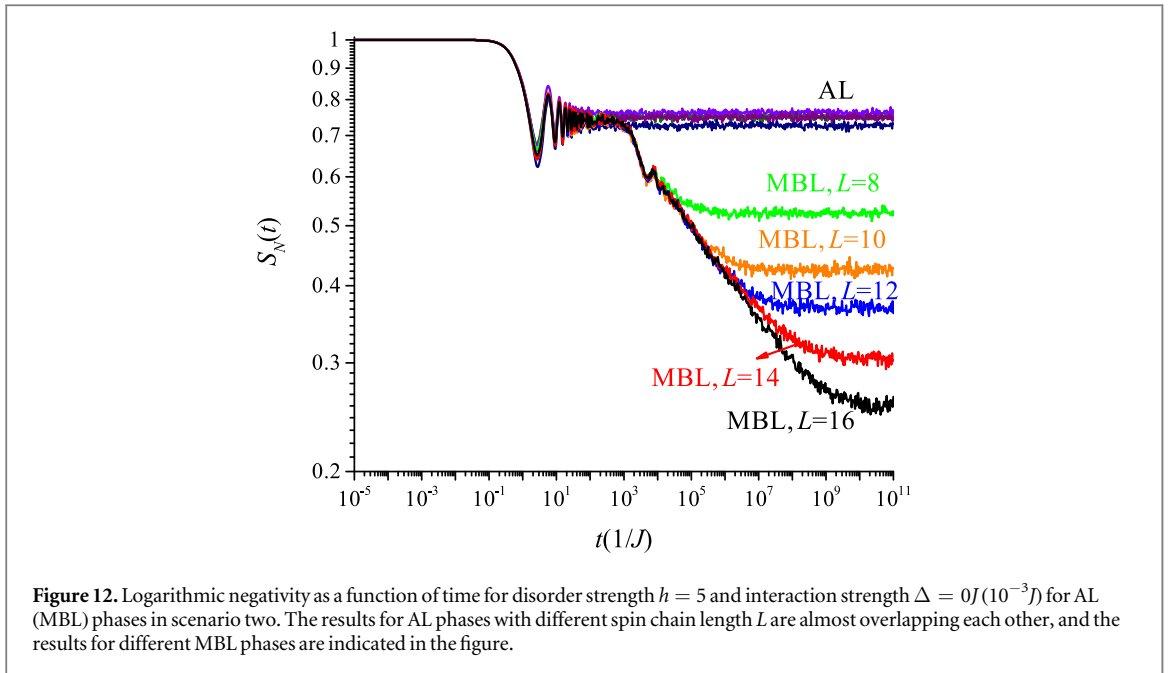
It is well known that von Neumann entropy is not a valid entanglement measurement if the collective states are in mixed states. However, several entanglement measurements have been found for a pair of qubits, including concurrence, negativity and their close relatives: the entropy of formation and logarithmic negativity. These entanglement measurements are ‘good’ in the following sense: (i) for a maximally entangled state, i.e. an EPR pair, these measurements reach their maximum values (equal one in our definitions); (ii) for collective separable states, these measurements vanish; (iii) is a continuous function of density matrices of the two-qubit states. Notice that these measurements, however, do not necessarily give same ordering for different entangled states.

Let us first give the definition of the entanglement measurements mentioned above. Denoting the collective state for two selected qubits by a density matrix ρ , the concurrence is given by $C = \max(\sqrt{\lambda_1} - \sqrt{\lambda_2} - \sqrt{\lambda_3} - \sqrt{\lambda_4})$, where λ_i 's are the eigenvalues of $\rho\tilde{\rho}$ in descending order and $\tilde{\rho} \equiv \sigma^y \otimes \sigma^y \rho^* \otimes \sigma^y$. Concurrence is monotonically related to the entanglement of formation by the Wootters formula $S_F = h[(1 + \sqrt{1 - C^2})/2]$, where $h(x) = -x \log_2 x - (1 - x) \log_2 (1 - x)$. Negativity is a measure related to the Peres–Horodecki criterion: $N = 2 \sum_i \max(0, -\mu_i)$, where μ_i 's are the eigenvalues of ρ^Λ who is the partial transpose of ρ . The logarithmic negativity is then given by $S_N = \log_2(N + 1)$.

We show the time evolution of logarithmic negativity between a pair of qubits that initially prepared to be as an EPR pair in scenario one in the main text. Here, in the figures 9–12, we present results of other entanglement measures in scenario two and show that these measurements are qualitatively similar, and serve the same role in our analysis. Therefore, the discussions and conclusions of logarithmic negativity in scenario one are also applicable for all measurements in scenario two.

Appendix C. Quantum decoherence

Inspired by [33], we also study the decoherence of a spin in both AL and MBL phase. Without loss of generality, we initialized the second spin to the left in the chain (namely spin A) in a superposition state $|+\rangle = (|\uparrow\rangle + |\downarrow\rangle)/\sqrt{2}$, and all the other spins in a Nel's state. The quantum decoherence D can be quantified



by the absolute value of the off-diagonal density matrix element of spin A, which is then at the maximum value of 0.5 initially. The dynamical evolution of quantum coherence can be studied similarly to the spin echo scheme in [33]. However, instead of focusing on the canceling of time evolution by applying a time-reversal π -pulse, we study the decoherence directly by first applying a $\pi/2$ -pulse to the spin A at an initial time, and another $\pi/2$ -pulse before measuring the decoherence D . The result is present in figure 13. One key difference between the behavior of quantum decoherence and quantum entanglement is the fact that quantum decoherence in both AL and MBL phase decrease and saturated to a finite value in the thermodynamic limit $L \rightarrow \infty$, where quantum entanglement will eventually vanish in MBL phase. This can be understood as the quantum coherence is not sensitive to the dephasing in the system, and hence cannot distinguish the differences between AL and MBL phase.

ORCID iDs

Jia Wang  <https://orcid.org/0000-0002-9064-5245>

References

- [1] Ekert A K 1991 *Phys. Rev. Lett.* **67** 661
- [2] Bennett C H, Brassard G, Crépeau C, Jozsa R, Peres A and Wootters W K 1993 *Phys. Rev. Lett.* **70** 1895
- [3] Bennett C H, Brassard G, Popescu S, Schumacher B, Smolin J A and Wootters W K 1996 *Phys. Rev. Lett.* **76** 722
- [4] Horodecki M, Horodecki P and Horodecki R 1998 *Phys. Rev. Lett.* **80** 5239
- [5] Anderson P W 1958 *Phys. Rev.* **109** 1492
- [6] Basko D M, Aleiner I L and Altshuler B L 2006 *Ann. Phys., NY* **321** 1126
- [7] Altman E and Vosk R 2015 *Annu. Rev. Condens. Matter Phys.* **6** 383
- [8] Nandkishore R and Huse D A 2015 *Annu. Rev. Condens. Matter Phys.* **6** 15
- [9] Schreiber M, Hodgman S S, Bordia P, Lueschen H P, Fischer M H, Vosk R, Altman E, Schneider U and Bloch I 2015 *Science* **349** 842
- [10] Bordia P, Luschen H P, Hodgman S S, Schreiber M, Bloch I and Schneider U 2016 *Phys. Rev. Lett.* **116** 140401
- [11] Choi J-y, Hild S, Zeiher J, Schauss P, Rubio-Abadal A, Yefsah T, Khemani V, Huse D A, Bloch I and Gross C 2016 *Science* **352** 1547
- [12] Smith J, Lee A, Richerme P, Neyenhuis B, Hess P W, Hauke P, Heyl M, Huse D A and Monroe C 2016 *Nat. Phys.* **12** 907
- [13] Oganesyan V and Huse D A 2007 *Phys. Rev. B* **75** 155111
- [14] Atas Y Y, Bogomolny E, Giraud O and Roux G 2013 *Phys. Rev. Lett.* **110** 084101
- [15] Berkelbach T C and Reichman D R 2010 *Phys. Rev. B* **81** 224429
- [16] Pekker D, Refael G, Altman E, Demler E and Oganesyan V 2014 *Phys. Rev. X* **4** 011052
- [17] Agarwal K, Gopalakrishnan S, Knap M, Müller M and Demler E 2015 *Phys. Rev. Lett.* **114** 160401
- [18] Huse D A, Nandkishore R, Oganesyan V, Pal A and Sondhi S L 2013 *Phys. Rev. B* **88** 014206
- [19] Bahri Y, Vosk R, Altman E and Vishwanath A 2015 *Nat. Commun.* **6** 7341
- [20] Bauer B and Nayak C 2013 *J. Stat. Mech.* **2013** P09005
- [21] Chandran A, Khemani V, Laumann C R and Sondhi S L 2014 *Phys. Rev. B* **89** 144201
- [22] Luitz D J, Laflorencie N and Alet F 2015 *Phys. Rev. B* **91** 081103
- [23] Li X, Ganeshan S, Pixley J H and Sarma S D 2015 *Phys. Rev. Lett.* **115** 186601
- [24] Baygan E, Lim S P and Sheng D N 2015 *Phys. Rev. B* **92** 195153
- [25] Žnidarič M, Prosen T and Prelovšek P 2008 *Phys. Rev. B* **77** 064426
- [26] Kjäll J A, Bardarson J H and Pollmann F 2014 *Phys. Rev. Lett.* **113** 107204
- [27] Bardarson J H, Pollmann F and Moore J E 2012 *Phys. Rev. Lett.* **109** 017202
- [28] Serbyn M, Papić Z and Abanin D A 2013 *Phys. Rev. Lett.* **110** 260601
- [29] Deng D-L, Li X, Pixley J H, Wu Y-L and Sarma S Das 2017 *Phys. Rev. B* **95** 024202
- [30] Huang Y, Zhang Y-L and Chen X 2017 *Ann. Phys.* **529** 1600318
- [31] Chen X, Zhou T, Huse D A and Fradkin E 2017 *Ann. Phys.* **529** 1600332
- [32] Fan R, Zhang P, Shen H and Zhai H 2017 *Sci. Bull.* **62** 707
- [33] Serbyn M, Knap M, Gopalakrishnan S, Papić Z, Yao N Y, Laumann C R, Abanin D A, Lukin M D and Demler E A 2014 *Phys. Rev. Lett.* **113** 147204
- [34] Bahri Y, Vosk R, Altman E and Vishwanath A 2015 *Nat. Commun.* **6** 7341
- [35] Peres A 1996 *Phys. Rev. Lett.* **77** 1413
- [36] Horodecki M, Horodecki P and Horodecki R 1996 *Phys. Lett. A* **223** 1
- [37] Plenio M B 2005 *Phys. Rev. Lett.* **95** 090503
- [38] Fuchs G D, Burkard G, Klimov P V and Awschalom D D 2011 *Nat. Phys.* **7** 789
- [39] Fukuhara T, Hild S, Zeiher J, Schauß P, Gross C, Endres M and Bloch I 2015 *Phys. Rev. Lett.* **115** 035302
- [40] Jurcevic P, Lanyon B P, Hauke P, Hempel C, Zoller P, Blatt R and Roos C F 2016 *Nature* **511** 202
- [41] Martinez E A et al 2016 *Nature* **534** 516
- [42] Bera S and Lakshminarayan A 2016 *Phys. Rev. B* **93** 134204
- [43] Iemini F, Russomanno A, Rossini D, Scardicchio A and Fazio R 2016 *Phys. Rev. B* **94** 214206
- [44] De Tomasi G, Bera S, Bardarson J H and Pollmann F 2017 *Phys. Rev. Lett.* **118** 016804
- [45] Friesdorf M, Werner A H, Brown W, Scholz V B and Eisert J 2015 *Phys. Rev. Lett.* **114** 170505
- [46] Kim I H, Chandran A and Abanin D A 2014 Logarithmic entanglement lightcone in many-body localized systems arXiv:1412.3073
- [47] Huse D A, Nandkishore R and Oganesyan V 2014 *Phys. Rev. B* **90** 174202